



---

# Deliverable

## D2.10 Report on the temporal change of the upper crust properties using ambient noise techniques:

Deliverable information	
<b>Work package</b>	[WP2]
<b>Lead</b>	[UGA]
<b>Authors</b>	Laurent Stehly and Estelle Delouche, University Grenoble Alpes
<b>Reviewers</b>	[Ian Main as WP2 leader]
<b>Approval</b>	[Management Board]
<b>Status</b>	[final]
<b>Dissemination level</b>	[Public]
<b>Delivery deadline</b>	[28.02.2022]
<b>Submission date</b>	[21.02.2022]
<b>Intranet path</b>	[DOCUMENTS/DELIVERABLES/File Name]



Table of contents

**Summary.....3**

**1. Spatio temporal evolution of the upper crust in Italia associated with the 2016 Amatrice/Visso/Norcia Earthquakes.....4**

1.1 data used and processing.....4

1.1.1 data used.....4

1.1.2 data processing and noise correlations.....6

1.1.3 computing  $dv/v$  using the stretching method.....7

1.2 Temporal evolution of the seismic velocities in the upper crust in the Amatrice - Visso -Norcia area.....7

1.3 Temporal evolution of the seismic velocities in the upper crust in selected sub-regions.....8

1.4 Spatio temporal evolution of the upper crust from 2015 to 2017.....14

1.5 Conclusion.....15

**2. Temporal evolution of the upper crust in Greece and around the Gulf of Corinth from 2015-2020.....17**

2.1 Data and processing.....17

2.2 Exemple of  $dv/v$  at the station CL.MALA.....20

2. 3. Seasonal variations of the seismic velocities in Greece.....20

2.4  $dv/v$  seasonality map.....21

2.5 Can the seasonal variations of  $dv/v$  be explained by thermoelastic effect ?.....21

2.6 Can the seasonal variations of  $dv/v$  be explained by rainfalls ?.....22

2.7 Conclusion.....24

**Conclusion and futur work.....25**

**References.....26**

## Summary

The long term goal of this project is to monitor the spatio-temporal evolution of the mechanical properties of the crust associated with seismic events in Central Italy and Greece which are among the most seismic areas in Europe.

Indeed, identifying precursory changes to large magnitude earthquakes and thus to predict them is one of the main long term goals of seismology. Earthquakes occur on fault systems as a consequence of long-term strain accumulation and transient triggering mechanisms. However, our current understanding of the preparation, nucleation of earthquakes and their consequences on the crustal properties are still limited.

In recent years, geodetic methods such as GPS and InSAR have shown to be efficient to study the strain dynamics of the surface of the Earth in the vicinity of active faults. Over the last 15 years, the use of seismic ambient noise correlations has opened up a new way to monitor seismic wave velocity changes associated with earthquakes (Wegler & Sens-Schonfelder 2007; Brenguier et al. 2008; Chen et al. 2010; Zaccarelli et al. 2011; Froment et al. 2013). The method used in these studies has consisted of repeatedly extracting the Green's function of the medium between (ideally) pairs of receivers of a dense network by correlating the ambient noise records. Seismic wave speed changes within the medium can be monitored by analyzing the coda part of the reconstructed Green's function (Stehly et al. 2008). By using seismic noise correlation filtered in different period bands, different depth can be monitored ranging from a few meters (Sens-Schönfelder & Wegler, 2006, Hillers et al, 2015) down to the mid and lower crust (Froment et al., 2013, Rivet et al., 2013, Obermann et al., 2014; , Wang et al., 2019).

Thanks to these methodological advances, in active fault areas, it is nowadays accepted that the seismic velocities change within the upper crust as a result to stress change that relate to fluid circulation and to the modification of crack properties that can occur for instance during coseismic slip of large earthquakes (Brenguier et al., 2008). Indeed, stress changes and relaxation following earthquakes produce coseismic and postseismic processes. The study of postseismic processes is crucial to an understanding of the local rheology and mechanical properties of the crust and earthquake interactions.

However, the evolution of the seismic waves speed in the crust is not only related to earthquakes and tectonic processes and can also results from environmental change such as the response of the soil and the upper crust to thermoelastic perturbation (Meier et al., 2010 ) and rainfall for instance (Wegler et al., 2016, Poli et al., 2020, Barajas et al., 2021). Hence, in highly seismic regions such as Italy and Greece, an important issue is to be able to distinguish between crustal velocity variations due to tectonic processes and those due to environmental parameters.

The first part of the present report, is devoted to the study of the seismic wave velocity variations between 2015 and 2017 in Italy. We focused on this period in order to study specifically the Amatrice/Visso/Norcia earthquake sequence. We present maps of the seismic wave velocity variations at different dates highlighting the effects of the Amatrice and Visso/Norcia earthquakes on the upper crust and the post-seismic relaxation.

The second part of this report is devoted to Greece. We study the evolution of the seismic wave velocity in the upper crust between 2015 and 2020. Over a large area of Greece, our measurements are dominated by seasonal changes related to environmental parameters. In order to distinguish the changes related to tectonic processes from environmental parameters we investigate the origin of these seasonal changes. We show that in the Gulf of Corinth they can be explained by precipitation. This result remains to be generalized to the whole of Greece, in order to be able to study specifically the velocity changes associated with seismicity.

## 1. Spatio temporal evolution of the upper crust in Italia associated with the 2016 Amatrice/Visso/Norcia Earthquakes

The 2016 Amatrice/Visso/Norcia earthquakes sequence occurred within the Apennines mountain ranges in Central Italy in an area located approximately between the epicenter of the 6 April 2009 Mw 6.3 L'Aquila Earthquake located 30 km in the south and and the 1997–1998 Umbria-Marche seismic sequence. It caused about 300 fatalities and widespread damages in nearby villages.

From a methodological point of view, it is a particularly interesting sequence of earthquakes since it one of the few examples of large magnitude earthquakes that occurred within a dense seismic network. It provides thus a unique opportunity to image the co-seismic changes induced by the earthquakes, to study the long-term recovery of the crust and to attempt and to look for possible precursory changes in the medium that could have occurred before the mainshocks.

Three main shocks took place in 2016: The Mw 6.1 Amatrice earthquakes occurred on August 24. It was followed by Mw 5.7 Visso earthquakes on October 26 and the Mw 6.5 Norcia earthquakes on October 30. These three earthquakes occurred on southwest-dipping fault segments with a normal mechanism. More than 18,000 aftershocks have been identified with more than 20 events having magnitude greater than four.

The Amatrice/Visso/Norcia sequence of earthquakes is a particularly interesting test case to assess the possibility to use seismic noise correlations to identify precursory changes in the medium that could have occurred before one of the main shock. For example, Chiarabba et al. 2020, by performing seismic tomography in different time window have demonstrated an increase in P-wave velocity during a 2-months long preparatory phase before the Mw 6.5 Norcia earthquakes, followed by an abrupt velocity reduction due to accelerated creep close to the hypocenter that occurred a few weeks or days before the rupture.

### 1.1 Data used and processing

#### 1.1.1 Data used

We use continuous noise records on the vertical components of all publicly available permanent broadband seismic stations in Italy from January 2015 to December 2017. This includes the data of more than 200 of broadband seismic stations from the Italian Network operated by INGV and the Mediterranean Broadband Seismographic Network (Figure 1).

The stations used are ideally distributed across Italy with a higher density around central Italy where the 2016 earthquakes sequence occurred. This makes this data set particularly well suited to study the evolution of the seismic wave speed with a decent spatial and temporal resolution (Figure 2).

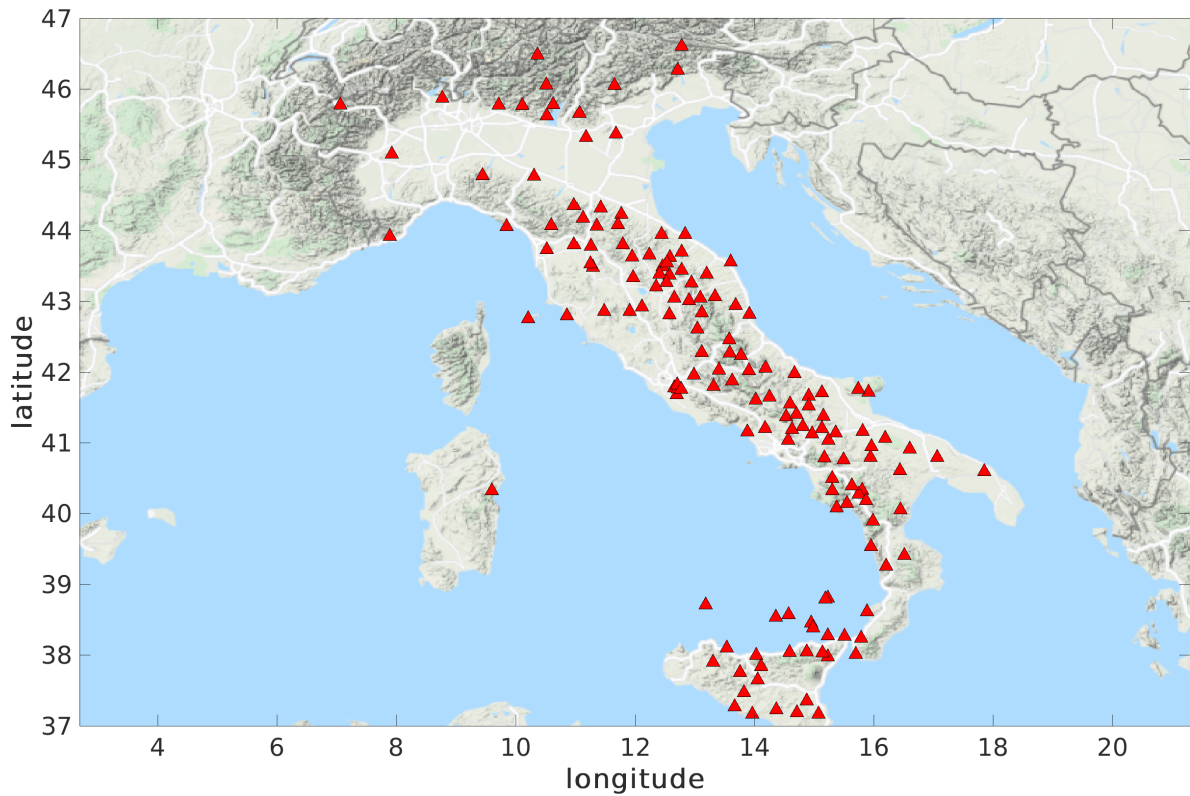
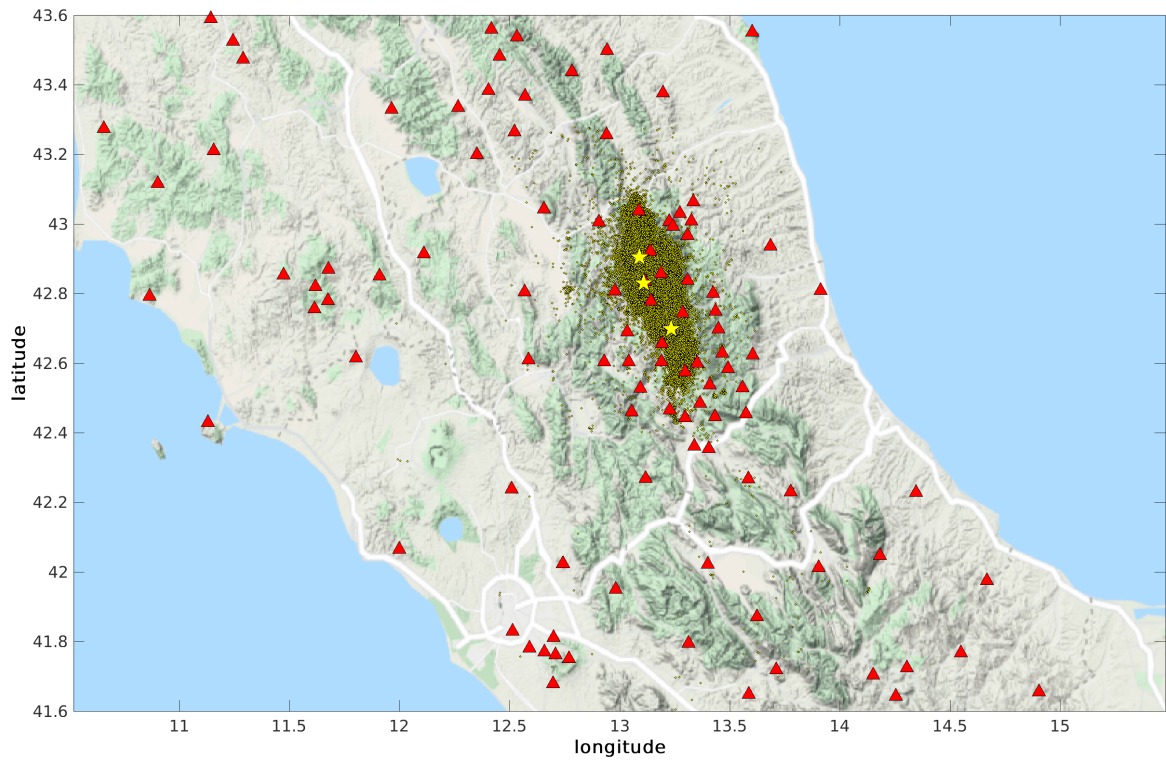


Figure 1: Map of Italy showing the broadband seismic stations (red triangles) used to measure the temporal evolution of the seismic velocities.



Figure

2: Map of the central Apennines showing the the broadband stations used to measure the temporal evolution of the seismic velocities (red triangles), the location (from south to north) of the August 24 Mw 6.1 Amatrice earthquakes, the october 30 Mw 6.5 Norcia earthquake and the october 26 Mw 5.7 Visso earthquake (yellow stars) and the location of aftershocks (yellow dots).

### 1.1.2 Data processing and noise correlations

We processed the noise records in the following way: first, the data were corrected for the instrumental response and decimated to a sampling frequency of 5 Hz. To downweight the contribution of energetic signals, such as glitches, earthquakes or oceanic storms, we normalized the amplitude of the records in the time domain, by dividing them by their envelope in the 1-3 s period band.

For each station pair, we cross-correlated the normalized vertical records day by day. In the following, we consider that these correlations are an approximation of the Green's function between the stations. Instead of analyzing these daily correlations, we consider 10 or 90-day-stacked correlations to increase the signal-to-noise ratio. The n-day-stacked correlations were computed by stacking the daily correlations with a sliding window of n days that is shifted by one day.

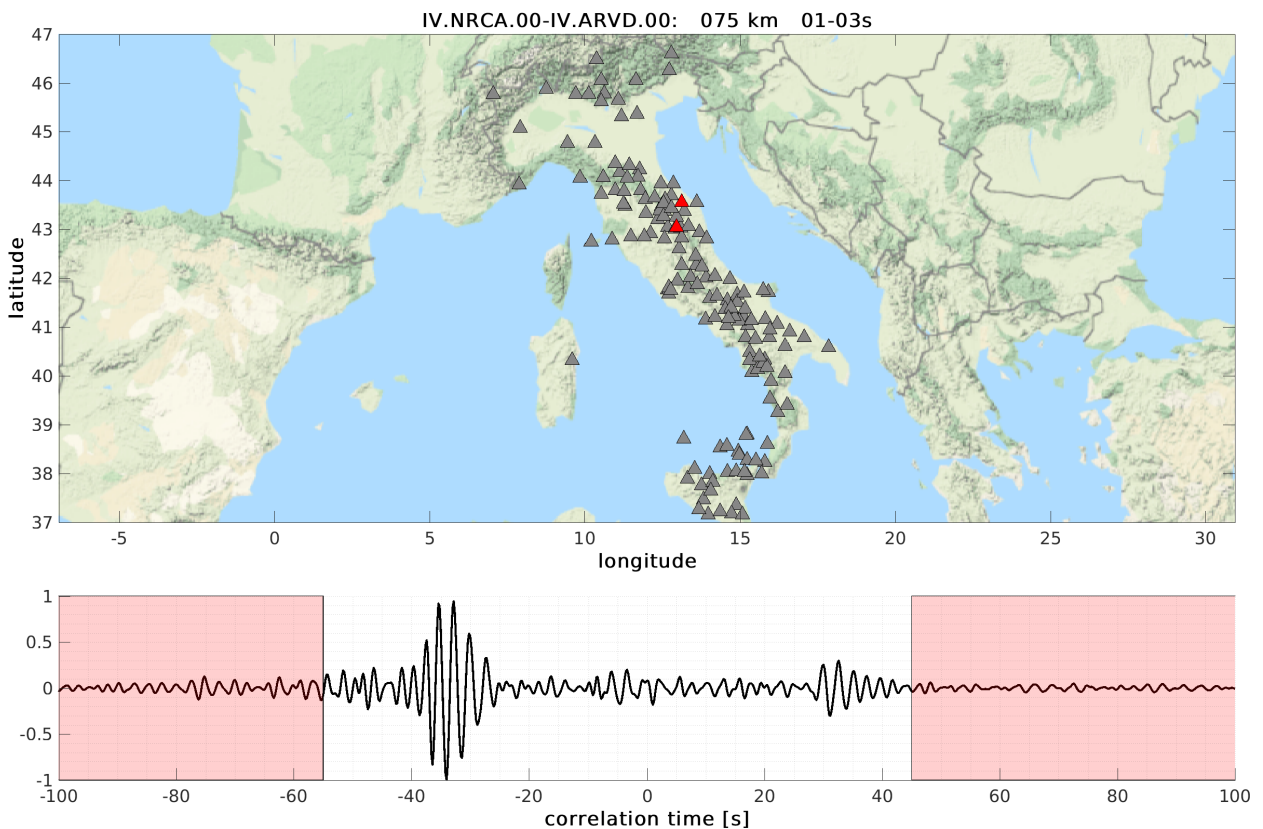


*Figure 3: Upper panel : map of Italy showing the broadband stations used for this study (gray triangles) and the two stations for which we show the correlation in the lower panel (red triangle).*

*Lower panel : example of noise correlation computed between the stations IV.NRCA.00 and IV.ARVD.00 averaged from 2015 to 2017. The coda waves used to measure the temporal evolution of the seismic velocities ( $dv/v$ ) are shown in the two red boxes.*

An example of the seismic correlation averaged over the period 2015 - 2017 between the stations IV.NRCA and IV.ARVD is shown on Figure 3. These two stations separated by 75 km are located in central Italy (Figure 3, upper panel). The correlogram is band passed filtered in the 1-3s period band. The Rayleigh wave propagating from IV.ARVD to IV.NRCA is clearly visible with a high signal-to-noise ratio in the negative correlation time around -35s, whereas the Rayleigh wave propagating the other way around is visible in the positive correlation time with a lower amplitude. The difference of amplitude between the Rayleigh waves in the positive and negative correlation time indicates that the seismic noise wavefield is not completely isotropic and has some directionality. However, to study the temporal evolution of the medium we will not use the direct waves that propagate between the stations. Instead we use coda waves in the time

window shown with shaded colors on Figure 3. Indeed coda waves are more sensitive to weak velocity changes since they spend more time in the medium.

### 1.1.3 Computing $dv/v$ using the stretching method

Our goal is to measure the temporal evolution of the seismic wave speed across Italy using noise correlations. In order to get the highest quality measurements we choose to use the stretching method which is less sensitive to noise in the data than the doublet method (Hadziioannou et al., 2011). This is particularly important since we would like to obtain the highest spatial and temporal resolution possible.

For each pair of stations, we first define a reference correlation which is the correlation averaged for the whole period 2015-2017. We then track medium changes by comparing each 10 - days or 90 - days correlations stack with the reference correlation. To that end, we use specifically the coda waves shown on Figure 3. Assuming a spatially homogeneous change in the medium velocity, the time delay of seismic waves increases linearly with the propagation time. This implies that the coda waves part of the Green function measured between two stations after a homogeneous change in the medium is either stretched or compressed by a factor  $(1 \pm dv/v)$  with respect to the coda waves measured before the change.

The relative velocity change  $\delta v/v$  at a given date with respect to a reference period of time is thus the stretching coefficient by which the time axis of the trace at this given date has to be stretched or compressed to obtain the best correlation with the correlation averaged over the reference period of time (2015-2017 in our case).

Ideally, the time window analyzed to measure the  $dv/v$  should start after the direct Rayleigh waves arrivals and span up to the point where the coda disappears into the noise level. In the 1-3 s period band, we use the coda waves in a window starting at a travel time corresponding to the arrival time of the Rayleigh waves + 15s and last 120s (see Figure 3).

## 1.2 Temporal evolution of the seismic velocities in the upper crust in the Amatrice - Visso -Norcia area

The temporal evolution of the coda wave speed in the 1-3 s period band in the areas where the 2016 Amatrice/Visso/Nocia sequence occurred is presented in Figure 4. We selected the stations shown in red on Figure 4 to perform this measurement. They are all located in a radius of 50 km around Norcia. As explained in the previous section the  $dv/v$  were computed between each pair of stations with a sliding window of 90 days in the 1-3s period band using the stretching method. The  $dv/v$  obtained between each pair of stations were then averaged to obtain the  $dv/v$  for this region (Figure 4 lower panel). This averaged  $dv/v$  is shown on the lower panel of Figure 4 with a black line. The gray shaded area indicates the error bars of the measurements. The red dotted line indicated the date of the Amatrice, Visso and Norcia earthquakes.

We find that from 2015 and 2017, the  $dv/v$  are between -0.04% and +0.02%. We find 3 main periods of time with distinct behaviors :

- From April 2015 to July 2016, the velocities are essentially stable with time. We note a small positive trend between April and December 2015, the  $dv/v$  varying from -0.015% to +0.02%, followed by a small decrease of velocity from December 2015 to July 2016. Further analysis are necessary to know if these trends are related to the internal dynamics of the crust, to external forcing, or to a seasonal change in the distribution of noise sources.
- From August 2016 to January 2017 we note a clear drop of the seismic velocity of 0.05% that is clearly associated with the Amatrice/Visso/Norcia earthquakes sequence. Despite the limited temporal resolution of 90 days, we note that the drop of velocity seems to

start around the date of the Visso/Norcia earthquakes that occurred in October 2016. On the other hand we do not note a clear change of velocity associated with the Amatrice earthquake which occurred on August 24. This is a first indication that the Amatrice and Visso/Norcia events did not have the same consequences on the crust.

- From February to December 2017 to November 2017, we observe a long-term decay of the relative velocity perturbation. In other words, the seismic velocities slowly recover. This is similar to the observation of Brenguier et al., 2008 who studied the 2004 Parfield earthquakes. They interpreted this evolution of the seismic velocities as a signature of post-seismic stress relaxation.

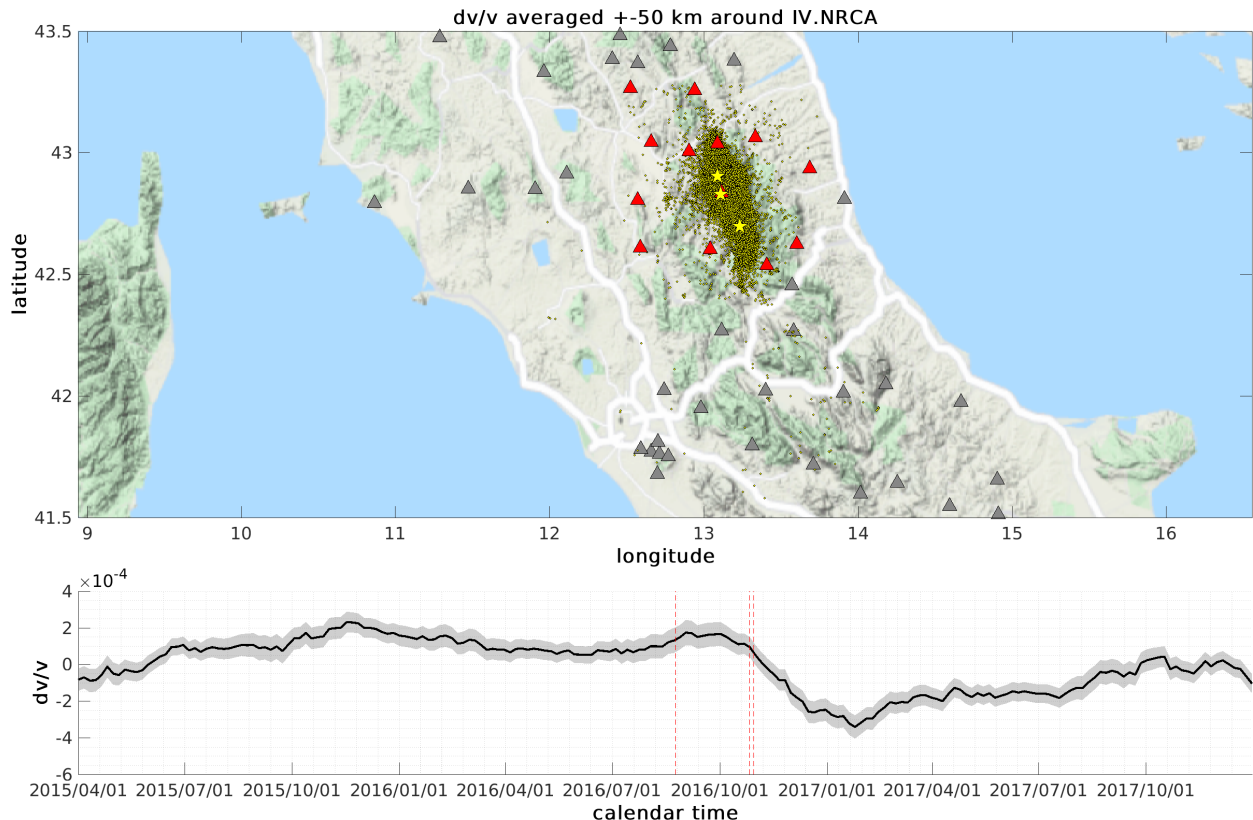


Figure 4: upper panel : map of central Italy showing the location of the broadband seismic stations used in this study (gray triangles), the stations used specifically to determine the temporal evolution of the seismic velocity in the region of Amatrice/Visso/Norcia (red triangles), the location (from south to north) of the August 24 Mw 6.1 Amatrice earthquake, the October 30 Mw 6.5 Norcia earthquake and the October 26 Mw 5.7 Visso earthquake (yellow stars) and the location of aftershocks (yellow dots).

Lower panel : evolution of the seismic velocities ( $dv/v$ ) measured in a radius of 50 km around Norcia with a 90 days sliding window from April 2015 to December 2017 (black line) and the corresponding error bars (gray shaded area). The dates of the Amatrice/Visso/Norcia earthquake are shown with a red dashed line.

### 1.3 Temporal evolution of the seismic velocities in the upper crust in selected sub-regions

Figure 5 shows the  $dv/v$  obtained in the 1-3s period band with a 90-days sliding window in four regions : the Po Plain, Amatrice, Sora and around Mount Etna. More precisely we computed in the  $dv/v$  by selecting all stations in a radius of 50 km around the red stars shown on the Figure 5 maps.

We note immediately that the evolution of the seismic velocities depend on the considered region :

- In the Po Plain (Figure 5, upper panel) , the seismic velocities have a clear negative trend in the entire period 2015-2017. Such a negative trend has been observed by Barajas et al., 2021 in southern Italy in the Pollino region. They attributed it to an accumulation of underground water. We note that this negative trend is not linear, and that it increases following the Amatrice/Visso/Norcia sequence. This unexpected observation may indicate that this earthquake sequence had long range consequences.
- Around Sora (Figure 5, 3<sup>rd</sup> panel) on the other hand, the seismic velocity continuously increases from April 2015 to December 2017.
- Around Mount Etna (Figure 5, 4<sup>th</sup> panel), the seismic velocities evolve following a complex pattern: we observe a succession of velocity increases and decreases. These may be related to the internal dynamic of the volcano as well as to external forcing.

Overall, the seismic velocities in Italy have a spatio-temporal evolution that results from tectonic processes, volcanic activity and probably from environmental parameters (rainfall). Figure 5 suggests that the Amatrice/Visso/Norcia sequence may have had long range consequences up to the Po Plain. Hence in the next subsection we go further by mapping the velocity variations.

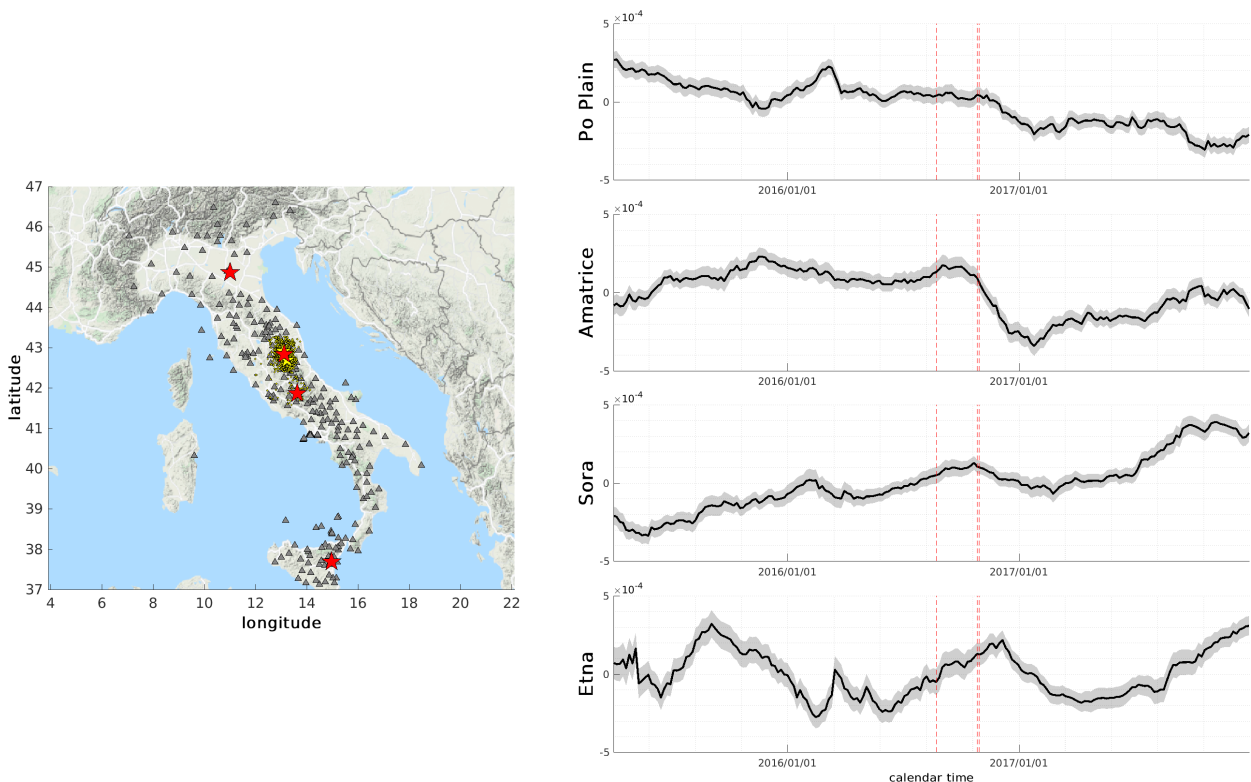


Figure 5: Left panel : map of Italy showing the location of the seismic stations used in this report (gray triangles) and the center of the four regions (red stars) for which we present the  $dv/v$  on the right panels.

Right panels : temporal evolution of the seismic velocity  $dv/v$  (black line) and its corresponding error bars (gray shaded area) measured in the 1-3s period band from 2015 to 2017 and averaged over a radius of 50 km in the Po Plain, around Amatrice, Sora, and the Mount Etna.

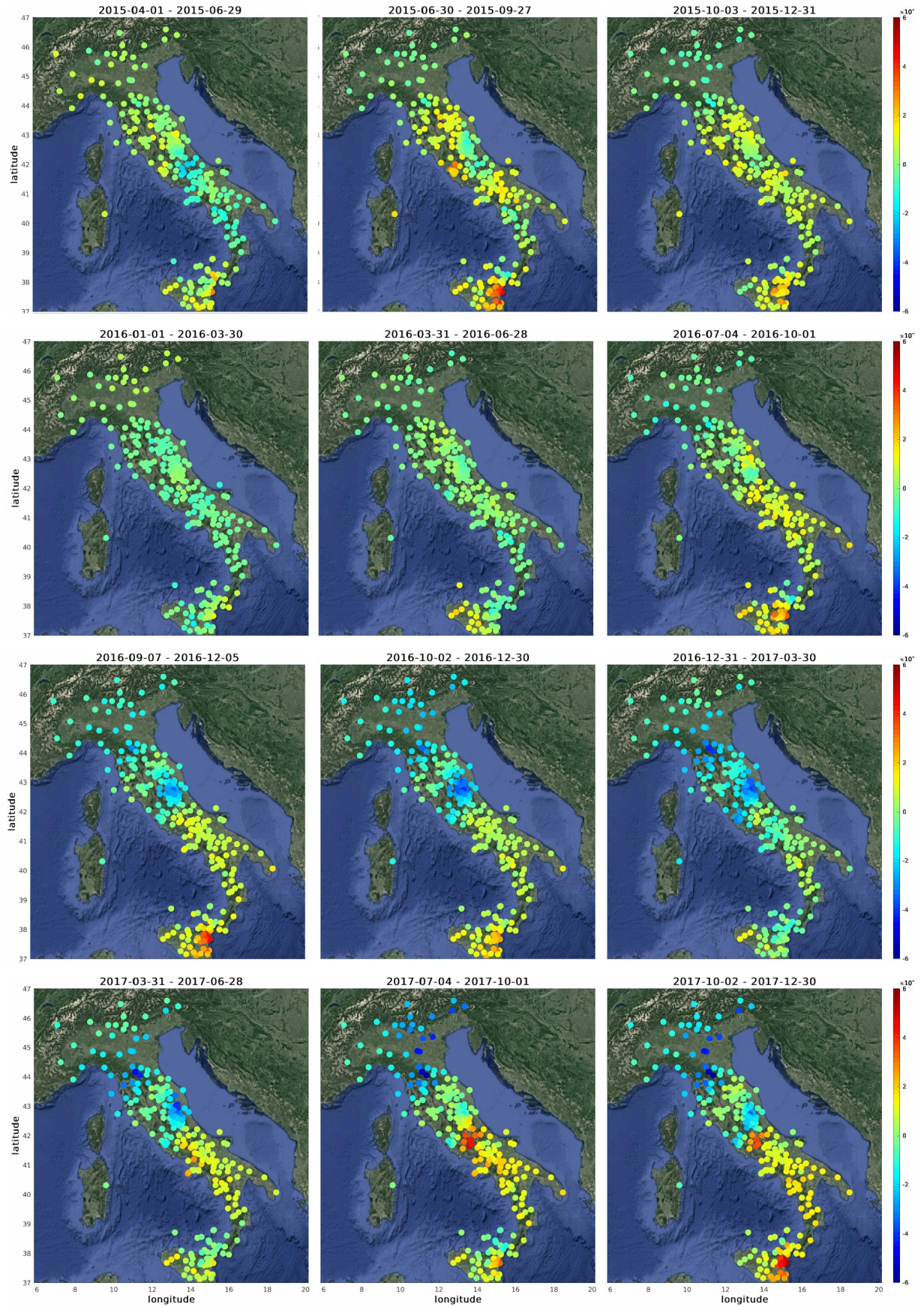


Figure 6:  $dv/v$  measured with a sliding window of 90 days around each station within a radius ranging from 50 to 200 km chosen to get at least 30 measurements. The  $dv/v$  maps are sorted by date from April 2015 to december 2017. We note a small drop of velocity of 0.02% associated with 24 august 2016 Amatrice earthquake and a more complex spatial pattern associated with Visso-Norcia sequence.

## 1.4 Spatio temporal evolution of the upper crust from 2015 to 2017

In the present subsection, we derive  $dv/v$  maps at different dates. Similarly to the previous section, we average the  $dv/v$  measured around each station in a radius ranging from 50 to 200 km determined so that there are at least 30 measurements (i.e 30 station pairs). The first months of 2016 are taken as the reference period. We then represent the averaged  $dv/v$  at the location of the central station

Figure 6 presents the results obtained from April 2015 to December 2017 with a window of 90 days and a similar colorbar going from -0.06% to +0.06%. We observe evidence of changes of seismic properties in the entire crust beneath Italy after the Amatrice/Visso/Norcia sequence of 2016 similar which remind the observation of Wang et al 2019 for Japan.

From April 2015 to June 2016 we do not observe any specific spatial or temporal pattern. The  $dv/v$  are close to 0 everywhere in Italy, with slightly negative value in the summer of 2015 in Central Italy and a positive value around central Italy.

With a 90-days sliding window, there is no obvious change of velocity associated with the 2016 Amatrice earthquake (August 24<sup>th</sup>) : in the time period 2016-07-04 to 2016-10-01 (figure 3, second line, 3<sup>rd</sup> column) we only observe a small drop of 0.02% around the Amatrice area and slight increase of velocity south to this area of 0.02%.

By contrast the consequence of the 2016 Visso/Norcia sequence is clearly visible (Figure 3, 3<sup>rd</sup> and 4<sup>th</sup> line). In the time period 2016-10-02 - 2016-12-30, we see a clear drop of velocity of 0.04% in a region of 100 km around the main shocks. There is no change of velocity in south to this area, however we observe a clear drop of velocity in the Po plain of 0.02%. This illustrates that the Visso/Norcia earthquakes may have affected the sediments of the Po Plain. The post-seismic relaxation is not homogenous, and in december 2017, the crust has not yet come back to its previous state (i.e 2016).

To better constrain the change of velocities specifically associated with the Amatrice/Visso/Norcia earthquakes we represent the  $dv/v$  obtained with a 10 days resolution in 2016 on Figure 7. Using a 10-days rather than a 90-days time window we get a better temporal resolution, but less precise  $dv/v$  measurements that need to be averaged over a greater radius to get a stable measurement. Thus we improve the temporal resolution at the expense of the spatial resolution.

On the upper panels of Figure 7, we represent the  $dv/v$  maps associated with the Amatrice earthquakes :

- In the window 2016-08-13 - 2016-08-22, that is from 11 days to 2 days before the Amatrice earthquake, we note an increase of velocity of 0.04% in Central Italy that extends to the west coast of Italy. We remind that the  $dv/v$  are measured taking the first month of 2016 as the reference.
- In the 2016-08-23 - 2016-09-01 window, that is from 1 days before the Amatrice Earthquake to 9 days after the main shock, we observe an increase of velocity south to Amatrice and a decrease of velocity north to Amatrice.
- In September 2016 the velocities come back to their previous state.

The  $dv/v$  maps associated with the Visso/Norcia sequence are presented on the lower panel of Figure 7. We observe a different pattern than for Amatrice :

- In the window 2016-10-17 - 2016-10-26, that is from 7 days before to day of the Visso event, we obtain a homogenous  $dv/v$  close to zero everywhere in Italy. This indicates that the seismic velocities are close to those of the reference period (first month of 2016).

- In the window 2016-11-01 – 2016-11-10, that is from 1 day to 10 day after the Norcia events, we measure a clear drop velocity of 0.02% in Central Italy close to the epicenter, but which is maximum in the Po Plain where it reach 0.04%. We note that in the Po Plain, there are fewer seismic stations, so the spatial resolution is less than 200 km, which may in turn lead to an over-estimate in the area where the velocity drop occurs.
- From November 2016 to December 2016, the seismic velocities come back progressively to their previous state.

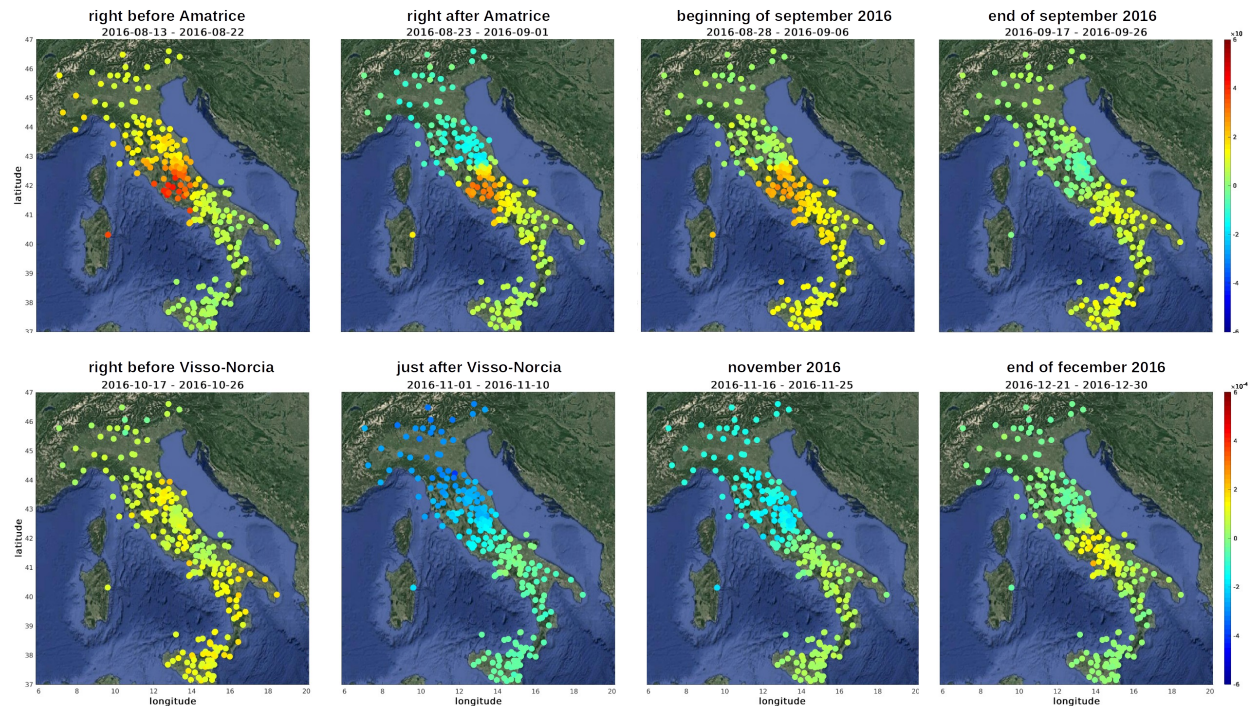


Figure 7:  $dv/v$  measured with a sliding window of 10 days around each station within a radius ranging from 50 to 200 km chosen to get at least 200 measurements. The upper panels present the velocity change measured just before and after the Amatrice earthquake. The lower panels present the velocity change measured just before and after the Visso-Norcia events.

## 1.5 Conclusion

Using seismic noise records at more than 200 broadband stations in Italy, we successfully mapped the spatial variations of the evolution of the seismic velocities ( $dv/v$ ), with a sliding window of 90 days and 10 days (Figure 6 and 7). We observe that the dynamic behaviour of the upper crust associated with the Amatrice earthquake and the Visso-Norcia sequence is different :

- The Amatrice event was preceded by an increase of velocity followed by a small decrease of velocity of 0.02% in the vicinity of the epicenter.
- The Visso/Norcia events were not preceded by a change of velocities but were associated with a velocity decreases that extend up to the Po Plain, followed by a long term recovery.

If it is clear that the Amatrice and Visso/Norcia earthquakes have generated a decrease in the seismic waves velocity of the order of 0.02% and 0.04% respectively in the fault zone, it is more difficult to interpret the other observations in particular the increase of velocity that occurred before the Amatrice earthquake in Central Italy. Indeed, the velocity changes may reflect the internal dynamics of the crust and be related to tectonic processes and seismicity, or

be due to external forcings such as environmental changes. Moreover, when data are analyzed with short time windows (typically less than 10 days) to obtain high temporal resolution, changes in the directionality of the seismic noise wavefield are more likely to bias the measurements.

To further interpret the  $dv/v$  maps it is crucial to be able to separate velocity variations due to tectonic processes from those due to environmental changes. This is what we investigate in the next section.

## 2. Temporal evolution of the upper crust in Greece and around the Gulf of Corinth from 2015-2020.

In this section we focus on the dynamics of upper crust in Greece with particular focus on the Gulf of Corinth. The long term goal of the work presented in this report is to monitor the spatio-temporal evolution of the mechanical properties of the crust around the Gulf of Corinth in Greece that are associated with seismic swarms and large magnitude ( $M_w > 5$ ) earthquakes, in order to 1) better understand the seismic cycle and 2) to look for possible change in the medium prior to large magnitude earthquakes.

We study Greece in addition to Italy for two reasons : first of all, Greece is one of the most seismic areas in Europe with more than 15000 earthquakes detected each year. This seismicity is expressed both in the form of discrete events and seismic crises caused by earthquakes swarms and main shocks that can have greater magnitude ( $M_w > 4$ ). Thus we aim at using seismic ambient noise to study the temporal evolution of the upper crust associated with seismicity.

Secondly, about one third of rocks exposed at the surface in Greece is made of relatively permeable carbonate and karst. This makes Greece an ideal area to study the impact of precipitation on the seismic waves velocities. This is particularly interesting for two reasons : we would like 1) to see if it is possible to use seismic noise to study the residence time of the water and its dynamics in the upper crust and 2) to determine what is the best strategy to correct the to correct the measured  $dv/v$  from the impact of the precipitation to keep only the velocity variations related to tectonic processes.

### 2.1 Data and processing

We used 6 years (2015-2020) of seismic noise recorded on the vertical component of 142 broadband seismic stations (figure 8). These stations belong to the corinth Rift Laboratory network, to the seismological network of Crete, the University of Thessaloniki, the university of Patras and the Hellenic seismic network (network code CL, HC, HT, HP, HL respectively).

Similarly to the work done in Italy as presented in the previous section, we computed daily noise correlations for each pair of stations. The evolution of the seismic waves velocities ( $dv/v$ ) was measured in the 1-3s period band with a sliding window of two months. Figure 9 shows an example of daily autocorrelations computed at the stations CL.AGRP and CL.MALA. We see clearly the coda waves in the -50s +50s time window that are used to compute the  $dv/v$ . The upper panels shows the matrix of daily auto-correlations calculated at stations CL.MALA and CL.AGRP. From day to day, we observe some random changes in waveforms. This is explained by the dynamics of the seismic ambient noise which evolves on a time scale of a few days. On the other hand, visually we do not see any change in arrival time in the coda that could correspond to changes in the environment. This confirms that if there are changes in the velocity of seismic waves they are necessarily of low amplitude. This justifies our choice to specifically for  $dv/v$  between -0.2 and +0.2% calculate the  $dv/v$  with the stretching method.

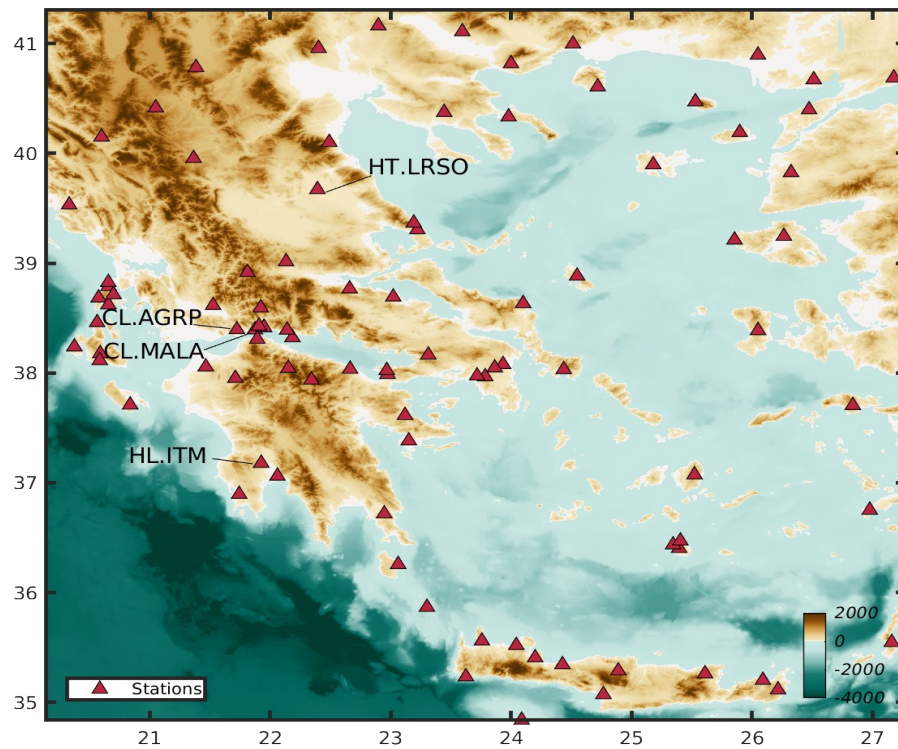


Figure 8: Map of Greece showing the broadband seismic stations (red triangles) used to measure the temporal evolution of the seismic velocities.

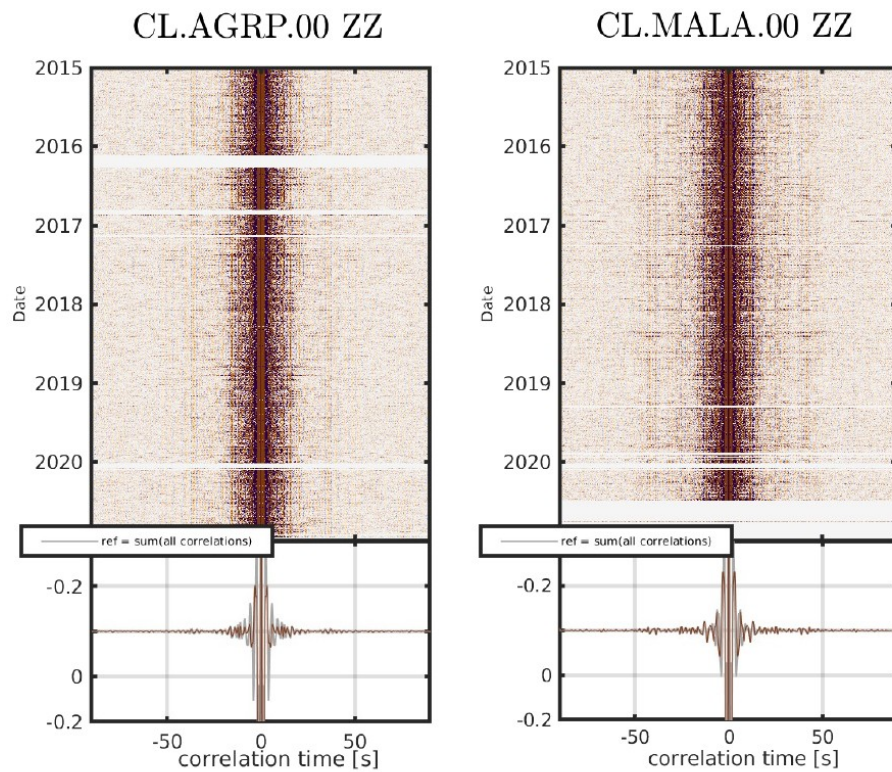


Figure 9: example of daily auto-correlations computed at the station CL.AGRP (left panel) and CL.MALA (right panel). The sum of all the daily correlations is shown on the lower panels. In addition to the central peak, coda waves are clearly visible between -50s and +50s for both stations

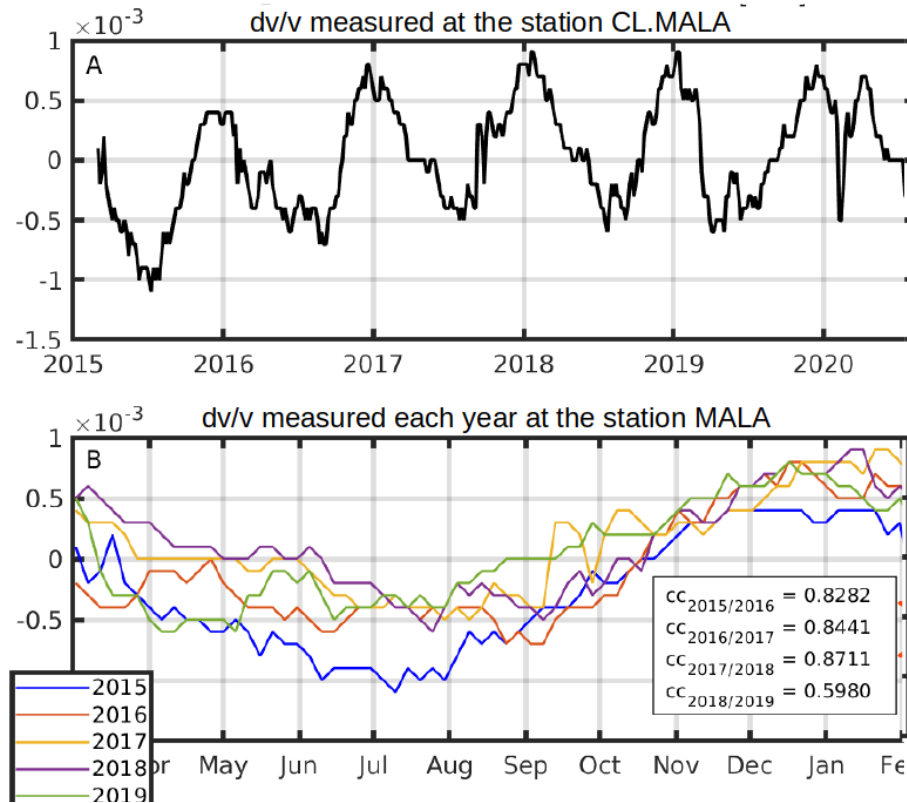


Figure 10: upper panel :  $dv/v$  computed at the station CL.MALA using seismic noise auto-correlations from 2015 to 2020 in the 1-3s period band with a sliding window of 60 days. Lower panel :  $dv/v$  computed each year from 2015-2020. The legend indicates the correlation coefficient between the  $dv/v$  measured each year and the previous one.

## 2.2 Example of $dv/v$ at the station CL.MALA

On Figure 10, we show the  $dv/v$  computed between 2015 and 2020 at the station MALA with a sliding window of 60 days and using auto-correlations filtered between 1 and 3s of period. The evolution of the seismic wave velocity is clearly dominated by seasonal variations with velocities increasing systematically by +0.02% in winter and decreasing by -0.02% in summer.

To further characterize these seasonal variations, we represent on the lower panel of Figure 10, the  $dv/v$  computed each year between 2015 and 2020. We notice that the velocity changes are similar each year, with the velocity increases and decreases occurring at the same period of year. To quantify these seasonal variations, we calculate the correlation coefficient between the  $dv/v$  calculated each year and the previous year. This correlation coefficient is greater than 0.82 between 2015-2016, 2016-2017, and equal to 0.60 between 2017-2018.

## 2.3. Seasonal variations of the seismic velocities in Greece

We observed that at the station CL.MALA, the  $dv/v$  are dominated by a clear seasonal pattern. In this section, we further attempt to characterize and understand the origin of these seasonal variations at the scale of Greece. Our long term goal is to distinguish the  $dv/v$  due to tectonics from those that are due to the influence of environmental parameters.

## 2.4 dv/v seasonality map

We determine in which region the  $dv/v$  are dominated by seasonal variations. To that end, we use the seismic noise auto-correlations calculated at each station to calculate the  $dv/v$  with sliding window of 60 days and between 1-3s period. We quantify the importance of the seasonal variations by calculating the average correlation coefficient between the  $dv/v$  calculated each year between 2015 and 2020. A value close to 1 indicates that the  $dv/v$  calculated each year are similar and thus dominated by seasonal variations. Conversely, low values indicate that the  $dv/v$  are not dominated by seasonal variations.

The results are presented on Figure 11. The colors of the map indicate the correlation coefficients obtained at each station. They were interpolated between each station. The main karst areas are indicated by the red circles. We note a first order correlation between the areas where seasonal variations are detected (correlation coefficient  $> 0.8$ ) and the distribution of karstic areas. This first-order correlation between the magnitude of seasonal variations in  $dv/v$  and the presence of karst is valid only for mainland Greece, but not on the island of Santorini for instance.

## 2.5 Can the seasonal variations of $dv/v$ be explained by thermoelastic effect ?

Any spatial gradient of the surface temperature field produces a thermoelastic strain that can affect the mechanical properties of the crust over typically in the first kilometer. For example, Ben-Zion & Allam, 2013 have shown that a temperature field with a wavelength of 3 km can produce a stress level of 10 kPa in first kilometer of the crust.

Assuming that the surface temperature changes with a period of one year, in an homogeneous elastic medium, the thermo-elastic strain and subsequently the change of the seismic waves velocity are delayed by  $\sim 45$  days with respect to the temperature fluctuation.

In order to test the hypothesis that surface temperature changes are the cause of seismic wave velocity variations, we use data from 495 weather stations (Figure 12). This allows us to quantify the time lag between temperature changes and seasonal variations of  $dv/v$ .

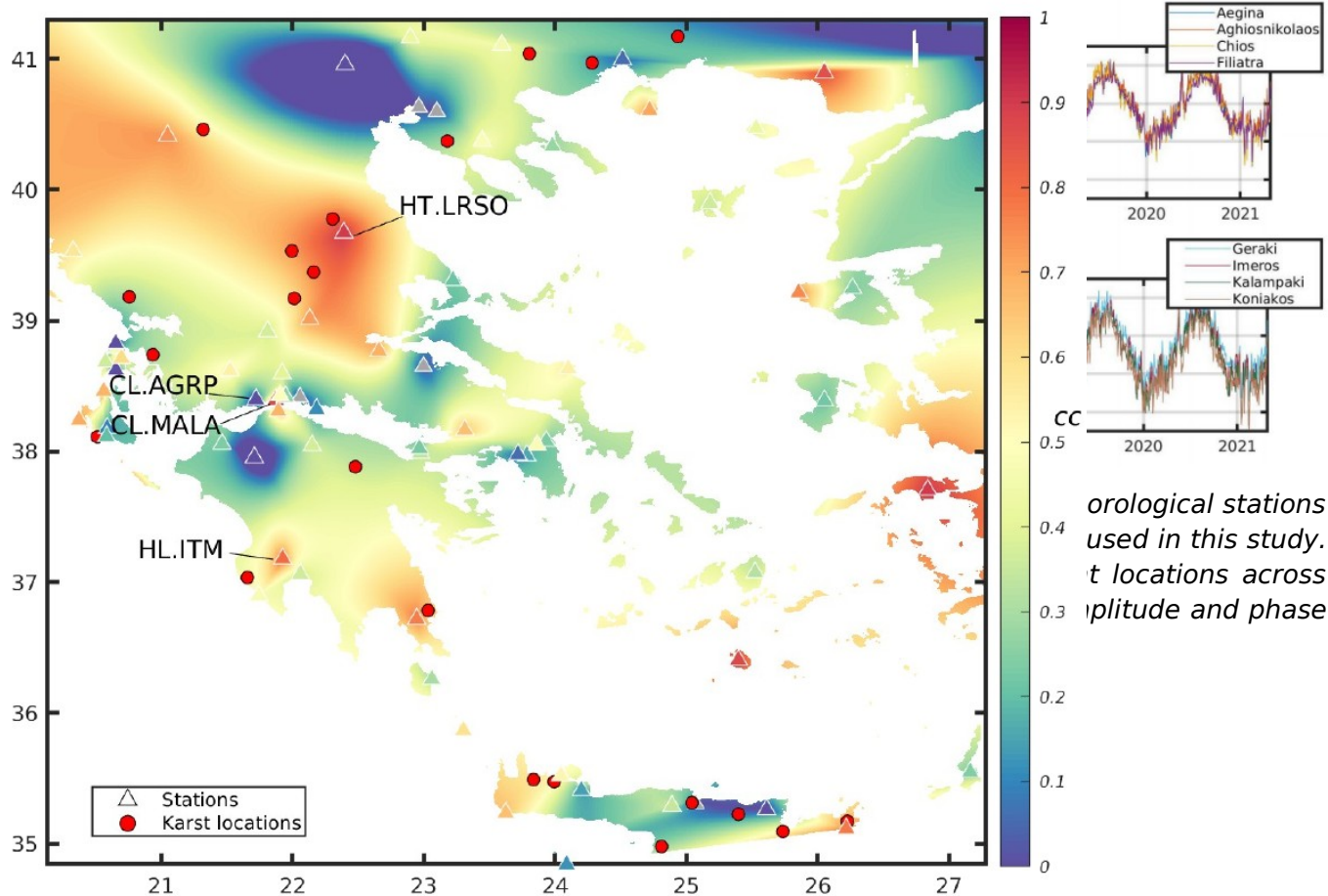


Figure 12:  $dv/v$  seasonality strength distribution : map of Greece showing the stations used in this study (red triangles) and the main karst of Greece (red circle). The color of the map represents the average correlation coefficient between the  $dv/v$  computed each year from 2015 to 2020 at each station using seismic noise auto-correlations. These average correlation coefficients obtained at each station are then interpolated. Value close to 1 indicates that the  $dv/v$  are similar each year i.e that they are dominated by seasonal variations. Low correlation coefficient indicates that no clear seasonal variations are detected.

Looking at the temperature recorded between 2015 and 2021 at 8 different meteorological stations spread all over Greece (Figure 12, right panels), we note that the temperature variations are similar at all stations in term of amplitude and phase, with the lowest temperature in January and the highest in July/August, the amplitude of the seasonal variations of temperature being between 20 and 30 degree.

On the contrary, the seasonal variations of the seismic wave velocity have different phases depending on the stations considered (Figure 13). For instance, at the station CL.MALA the velocity of seismic waves is maximal in January and minimum in August, while it is the opposite at the station HL.ITM (Fig 13, black and yellow line). Hence, depending on the station, the time lag between temperature variations and  $dv/v$  varies from 2 to 6 months. Such spatial variability makes it unlikely that seasonal variations in  $dv/v$  are due to solely temperature change.

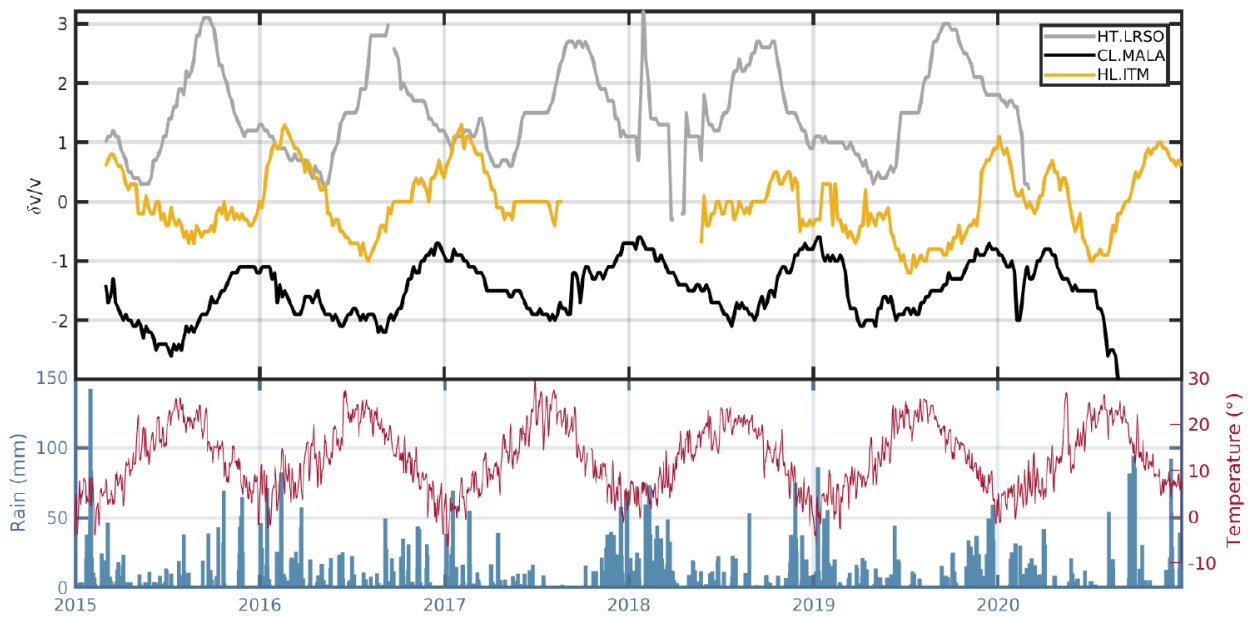


Figure 13:  $dv/v$  measured from 2015 to 2020 at the stations HT.LRSO (gray), CL.MALA (blue), and HL.ITM (yellow) on noise auto-correlations using a sliding window of 60 days in the 1-3s period band. Lower panel : temperature in degree and daily rainfall in mm at a meteorological station located in the Gulf of Corinth near CL.MALA

## 2.6 Can the seasonal variations of $dv/v$ be explained by rainfalls ?

In this section, we examine whether the observed velocity variations at the station CL.MALA can be better explained by precipitation. As shown on Figure 13, the largest precipitation around MALA occurs between November and January with daily precipitation often exceeding 10 mm/year. By contrast the rainfalls is low in the summer.

Rainfall can affect the seismic waves velocities through an elastic and poro-elastic response of the uppermost crust :

- the loading pressure exerted by the water can depress the surface leading to an elastic response of the subsurface.
- by increasing the pore-pressure of the subsurface, rainfall also induces a poroelastic response that can generate a rise in the surface. In this case the seismic waves velocity and the water pressure would be expected to be anticorrelated : an increase in the amount of water in the aquifer increases the pore pressure which reduce the overall effective pressure, hence reducing the seismic velocities.

To evaluate the poro-elastic effect on the seismic waves velocity, we apply a simple model to estimate the water levels in the subsurface following the work of Barajas et al., 2021. We assume that rainfall supplies water in the aquifer and that the flux of water from the aquifer to the surrounding is proportional to 1) the difference in the amount of water between inside and outside the considered aquifer and 2) the area of the border of the considered aquifer.

This implies that the aquifer loses water at a rate which is proportional to the water level (Fiorillo 2011, Barajas et al., 2021). The proportionality coefficient  $k$  is expressed in  $\text{day}^{-1}$  and represents the rate at which water flows out of the aquifer, i.e. it quantifies the capacity of the aquifer to "hold" water. Assuming a linear relationship between the  $dv/v$  and the water level inside the aquifer, it is possible to compute synthetic  $dv/v$  from rainfall. There is a single free parameter  $k$  which is determined through a simple gridsearch by minimizing the misfit between the observed and predicted  $dv/v$ .

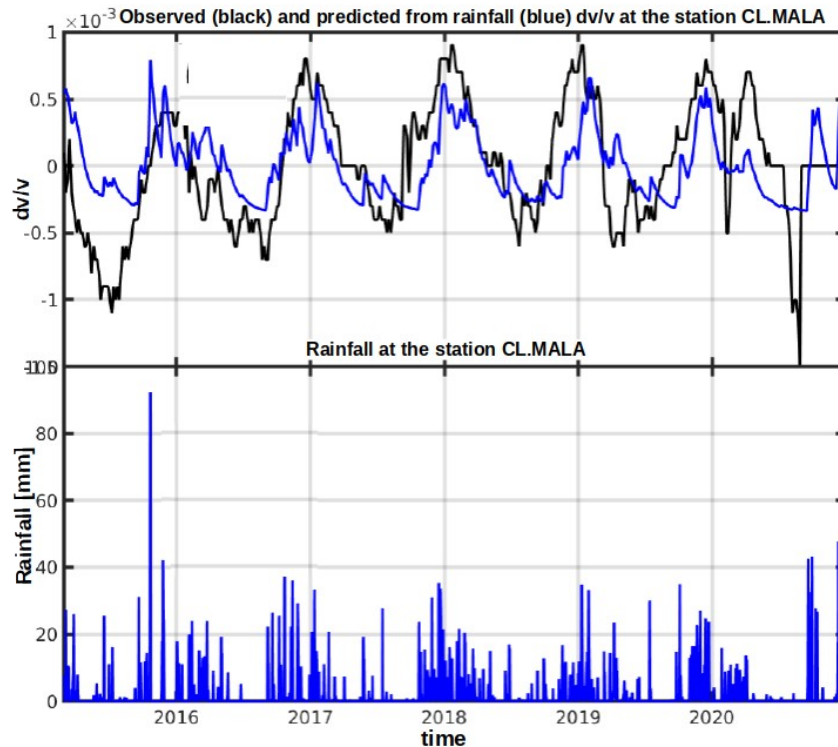


Figure 14: upper panel : observed (black) vs predicted from rainfall (blue)  $dv/v$  at the station MALA from 2015 to 2020. The observations are made in the 1-3s period band. Lower panel : daily precipitation in mm at the closest meteorological station to Mala from 2015 to 2020.

The results obtained at the station MALA located in the Gulf of Corinth (Figure 11) are shown in Figure 14. The bottom panel shows the daily precipitation in mm measured at the nearest meteorological station to MALA. These data were used to compute the variation of the seismic wave velocity due to rain-induced poroelastic response of the subsurface (blue), as explained in the previous paragraph. We compare it with the observed  $dv/v$  between 1-3s of period. We find a good agreement in general between the observed and synthetic  $dv/v$  for the optimal value of  $k$ . In particular, the seasonal variation of the synthetic and observed are similar in terms of amplitudes and phase. This confirms that for the MALA station located in the Gulf of Corinth, it is indeed possible to explain the seasonal variation of the seismic wave velocity by the precipitation and that this provides a better explanation for the observations than temperature alone. However we also observe some difference between the two that can be due to the elastic effect of rain which has not been modeled and/or to tectonic processes. Further investigations are needed to elucidate this point.

## 2.7 Conclusion

We are studying Greece in the framework of the Rise project since it is the most seismic region in Europe. Our aim is to determine the variations in seismic wave velocity related to tectonic processes, in order to look for potential precursory signals to large ( $M_w > 5$ ) magnitude earthquakes and to study the evolution of the mechanical properties of the crust associated with discrete earthquakes and seismic swarms.

We have seen that over large areas in Greece (Figure 11), the velocity of seismic waves changes with the season. We thus attempt to understand the origin of the seasonal variation in order to correct our measurements from environmental parameters and therefore to get the variations of seismic velocity related specifically to tectonic processes.

We think it is unlikely that seasonal temperature variations and associated thermoelastic effects can be at the sole origin of seasonal variations in seismic wave velocity, because the time lag between  $dv/v$  and temperature changes varying from 2 to 6 months (Figure 13) is too long to be explained by thermoelasticity. On the contrary, for the MALA station located in the Gulf of Corinth, a simple linear reservoir model estimates the water levels inside the aquifer which allows to predict the observed  $dv/v$ , showing that the velocity variations are inversely proportional to the pore pressure inside the aquifer. In other words, the poro-elastic response of the soil due to precipitation can explain a large part of the seasonal variations of the seismic wave velocity (Figure 14). We will attempt to confirm this result with GPS data, and to verify that the difference between observed and predicted  $dv/v$  can be explained by 1) elastic effects related to precipitation and 2) by tectonic processes. We then plan to see if at all the sites where seasonal variations of seismic waves are observed, these can be explained by precipitation in a similar way. If so, we will then be able to map the  $dv/v$  related to tectonic processes, by correcting our measurements for environmental effects.

## Conclusion and future work

During the first part of the RISE project, we built a database of background recordings covering all of Europe, and in particular Italy and Greece (RISE Milestone M2.5.1: Screening for ambient noise anomalies in test regions). By developing efficient data processing tools, allowing us to process several TB of data, we were able to systematically compute daily correlations between each pair of stations.

We focused on Italy and Greece and in particular the Gulf of Corinth, these regions being among the most seismic in Europe.

In order to study the spatio-temporal evolution of the mechanical properties of the crust, and to look for potential precursory changes in the medium prior to large magnitude earthquakes, we mapped the evolution of seismic wave velocity in Italy over the period 2015-2017 which includes the Amatrice-Visso-Norcia earthquake sequence. The results show that the velocity of seismic waves in the upper crust is not stable over time, but evolves on the scale of several weeks, with variations of the order of 0.1%, which is extremely small but nonetheless detectable above the noise using the cross-correlation method. The accuracy of the measurements depends on the time window used and the station density, so we are able to capture these variations with a temporal resolution of about 2 month. Some of these variations are clearly related to the Amatrice-Visso-Norcia sequence: this is the case of the co-seismic velocity drops followed by a co-seismic recovery visible in Central Italy.

We were able to highlight that the Amatrice earthquake is associated with a small velocity drop locally around the epicenter, while Visso-Norcia is associated with a larger velocity drop extending to the Po plain. Other seismic waves velocity variations are visible, however, further analysis are required to determine whether these variations are related to tectonic or environmental processes.

This motivated us to focus on Greece, which has a very strong seismicity and many relatively permeable karst regions that are susceptible to changes in properties by rainfall. Thus we found seasonal variations of seismic waves velocity more closely correlated to precipitation than temperature. Around the Gulf of Corinth we showed that it is possible to predict the observed seismic velocity variations from meteorological data.

At present our objectives are the following:

- We want to explore the possibility of predicting velocity variations related to environmental parameters from weather data, in order to distinguish between velocity variations related to tectonic and environmental processes. Here, the long term objective is to establish maps showing the seismic wave velocity variations in Italy and Greece related to tectonic processes only.
- We plan to study the velocity variations associated with seismic events and earthquake swarms in the Gulf of Corinth. The objective will be to use the earthquakes themselves as a source of noise in order to attempt to measure seismic wave velocity variations at high temporal resolution (<1 day) and see how these are related to the dynamics of the seismic swarms.
- We will also explore other frequency bands to study the behavior of the lower crust.

## References

- Brenguier, F.; Campillo, M.; Hadziioannou, C.; Shapiro, N. M.; Nadeau, R. M. & Larose, E. Postseismic Relaxation Along the San Andreas Fault at Parkfield from Continuous Seismological Observations *Science*, 008, 321, 1478-1481
- Brenguier, F.; Shapiro, N. M.; Campillo, M.; Ferrazzini, V.; Duputel, Z.; Coutant, O. & Nercessian, A. Towards forecasting volcanic eruptions using seismic noise, *Nature Geoscience*, 2008, 1, 126-130
- Ben-Zion, Y. & Allam, A.A., 2013. Seasonal thermoelastic strain and post-seismic effects in Parkfield borehole dilatometers, *Earth planet. Sci. Lett.*, 379, 120–126.
- Barajas, A.; Poli, P.; D'Agostino, N.; Margerin, L. & Campillo, M. Separation of Poroelastic and Elastic Processes of an Aquifer From Tectonic Phenomena Using Geodetic, Seismic, and Meteorological Data in the Pollino Region, Italy *Geochemistry, Geophysics, Geosystems*, 2021
- Brenguier, F.; Campillo, M.; Hadziioannou, C.; Shapiro, N. M.; Nadeau, R. M. & Larose, E. Postseismic Relaxation Along the San Andreas Fault at Parkfield from Continuous Seismological Observations, *Science*, 2008, 321, 1478-1481
- Brenguier, F.; Shapiro, N. M.; Campillo, M.; Ferrazzini, V.; Duputel, Z.; Coutant, O. & Nercessian, A. Towards forecasting volcanic eruptions using seismic noise *Nature Geoscience*, Nature Publishing Group, 2008, 1, 126-130
- Distribution of seismic wave speed changes associated with the 12 May 2008 Mw 7.9 Wenchuan earthquake *Geophysical Research Letters*, American Geophysical Union (AGU), 2010, 37
- Chiarabba, C.; De Gori, P.; Segou, M. & Cattaneo, M. Seismic velocity precursors to the 2016 Mw 6.5 Norcia (Italy) earthquake *Geology*, 2020, 48, 924-928
- Froment, B.; Campillo, M.; Chen, J. & Liu, Q. Deformation at depth associated with the 12 May 2008 MW 7.9 Wenchuan earthquake from seismic ambient noise monitoring *Geophysical Research Letters*, American Geophysical Union (AGU), 2013, 40, 78-82
- Hadziioannou, C.; Larose, E.; Baig, A.; Roux, P. & Campillo, M. Improving temporal resolution in ambient noise monitoring of seismic wave speed, *Journal of Geophysical Research*, American Geophysical Union (AGU), **2011**, 116
- Hillers, G.; Husen, S.; Obermann, A.; Planès, T.; Larose, E. & Campillo, M. Noise-based monitoring and imaging of aseismic transient deformation induced by the 2006 Basel reservoir stimulation *Passive monitoring of deformation Geophysics*, 2015, 80, KS51-KS68
- Meier, U.; Shapiro, N. M. & Brenguier, F. Detecting seasonal variations in seismic velocities within Los Angeles basin from correlations of ambient seismic noise *Geophysical Journal International*, 2010, 181, 985-996
- Obermann, A.; Froment, B.; Campillo, M.; Larose, E.; Planès, T.; Valette, B.; Chen, J. H. & Liu, Q. Y. Seismic noise correlations to image structural and mechanical changes associated with the Mw7.9 2008 Wenchuan earthquake *Journal of Geophysical Research: Solid Earth*, 2014, 119, 3155-3168

Stehly, L.; Campillo, M.; Froment, B. & Weaver, R. L., Reconstructing Green's function by correlation of the coda of the correlation (C3) of ambient seismic noise *Journal of Geophysical Research*, 2008, 113

Sens-Schönfelder, C. & Wegler, U. Passive image interferometry and seasonal variations of seismic velocities at Merapi Volcano, Indonesia *Geophysical research letters*, 2006, 33

Wegler, U. & Sens-Schönfelder, C. Fault zone monitoring with passive image interferometry *Geophysical Journal International*, 2007, 168, 1029-1033

Rivet, D.; Brenguier, F.; Clarke, D.; Shapiro, N. M. & Peltier, A. Long-term dynamics of Piton de la Fournaise volcano from 13 years of seismic velocity change measurements and GPS observations *Journal of Geophysical Research: Solid Earth*, 2014, 119, 7654-7666

Rivet, D.; Brenguier, F.; Clarke, D.; Shapiro, N. M. & Peltier, A. Long-term dynamics of Piton de la Fournaise volcano from 13 years of seismic velocity change measurements and GPS observations *Journal of Geophysical Research: Solid Earth*, 2014, 119, 7654-7666

Wang, Q.-Y.; Campillo, M.; Brenguier, F.; Lecointre, A.; Takeda, T. & Hashima, A. Evidence of Changes of Seismic Properties in the Entire Crust Beneath Japan After the Mw 9.0, 2011 Tohoku-oki Earthquake *Journal of Geophysical Research (Solid Earth)*, 2019, 124, 8924-8941

Zaccarelli, L.; Shapiro, N. M.; Faenza, L.; Soldati, G. & Michelini, A. Variations of crustal elastic properties during the 2009 L'Aquila earthquake inferred from cross-correlations of ambient seismic noise *Geophysical research letters*, 2011, 38

**Liability Claim**

The European Commission is not responsible for any that may be made of the information contained in this document. Also, responsibility for the information and views expressed in this document lies entirely with the author(s).